ECS Transactions, 39 (1) 155-162 (2011)
10.1149/1.3615189 ©The Electrochemical Society

Ballistic Transport Properties of Spin Field-Effect Transistors Built on Silicon and InAs Fins

D. Osintsev, V. Sverdlov, A. Makarov, and S. Selberherr

Institute for Microelectronics, TU Wien, Gußhausstraße 27-29, A-1040 Wien, Austria

We investigate the transport properties of ballistic spin field-effect transistors (SpinFET). We show that temperature exerts a significant influence on the device characteristics. For the InAs-based SpinFET an ambient temperature higher than T=150K leads to the absence of the ability to modulate the value of the tunneling magnetoresistance through changing the bandgap mismatch between the channel and the contacts. The length of the semiconductor channel impacts significantly the device characteristics. A shorter channel is preferred for potential operations at room temperature. For the silicon-based SpinFET the spin-orbit interaction has to be taken in the Dresselhaus form. We demonstrate that silicon fins with [100] orientation exhibit a stronger dependence on the value of the spin-orbit interaction and are thus preferable for practical realization of SpinFETs.

Introduction

The miniaturization of the feature sizes of semiconductor devices, or scaling, leads to the possibility to place more transistors on the same chip. A higher density of transistors on the chip allows increasing the computational speed of modern computers. However, scaling is rapidly approaching the fundamental physics limits. Besides, the present technology faces the problem of keeping the power dissipation under control while increasing the device density. This signifies that new engineering solutions have to be introduced in order to increase integration and computational speed while decreasing the power consumption in the future integrated circuits. A promising alternative to the electron charge degree of freedom currently used in MOSFET switches is to taking into account the electron spin. The spin of an electron possesses several exciting properties suitable for future devices. It is characterized by only two projections on a chosen axis – orientation up or down, and it can change its orientation rapidly by utilizing an amazingly small amount of energy. Thus exploiting electron spin properties in future microelectronic devices opens a great opportunity to achieve a performance which surpasses the one achieved in the present transistor technology.

The spin transistor is a switch which utilizes spin properties of electrons. We are following the proposal for a spin field-effect transistor (SpinFET) first made by Datta and Das (1). The SpinFET concept employs spin-orbit interaction in the channel to modulate the current through the device. SpinFETs are composed of two ferromagnetic contacts (source and drain), which sandwich the semiconductor channel region. The ferromagnetic source contact injects spin-polarized electrons in the semiconductor region. Because of the non-zero spin-orbit interaction the electron spin precesses during its propagation through the channel. Only the electrons with spin aligned to the drain magnetization can leave the channel through the drain contact, thus contributing to the current. The spin-orbit interaction is controlled electrically by applying an external gate voltage.

The total current through the device depends on the relative angle between the magnetization direction of the drain contact and the electron spin polarization at the end of the semiconductor channel. The spin precession angle $\Delta\theta$ defined as the difference between the orientation of the spin of the electron at the end and at the beginning of the semiconductor region is (2)

$$\Delta\theta = \frac{2\alpha\, m^*}{\hbar^2} L, \qquad [1]$$

where α is the strength of the spin-orbit interaction, m^* is the effective mass of the electron, $\hbar$ is the reduced Plack`s constant, and L is the length of the semiconductor channel. In the absence of the spin-orbit interaction the electrons propagate with their orientation conserved. The strength of the spin-orbit interaction determines the minimum length of the semiconductor channel, which will be sufficient to change the orientation of the spin to opposite. In case of the material with a strong spin-orbit interaction such as InAs the semiconductor channel will be shorter than for a material with weak spin-orbit interaction such as silicon.

Silicon is the main material used by semiconductor industry. Silicon possesses several exciting properties attractive for future spin-driven applications: it is predominantly composed of nuclei with zero spin and it is also characterized by a weak spin-orbit interaction. The spin relaxation in silicon is, therefore, relatively weak, which results in large spin life times (3), (4). In experiments, coherent spin propagation through an undoped silicon wafer of $350\mu m$ thickness was demonstrated (5). Coherent spin propagation over such long distances makes the fabrication of spin-based switching devices in the near future increasingly likely.

The two dominant mechanisms of spin-orbit interaction in III-V semiconductor heterostructures are of the Rashba and the Dresselhaus type. The Rashba spin-orbit interaction is due to the geometrically induced structural asymmetry (6) in the system. while the Dresselhaus spin-orbit interaction is caused by bulk inversion symmetry breaking (7). The effective Hamiltonian of the spin-orbit interaction due to the structurally induced inversion asymmetry (Rashba type) along the z-axis is in the form

$$H_R = \frac{\alpha_R}{\hbar}(p_x\sigma_y - p_y\sigma_x), \qquad [2]$$

where α_R is the effective electric field-dependent parameter of the spin-orbit interaction, $p_{x(y)}$ is the electron momentum projection, and σ_x and σ_y are the Pauli matrices. This is usually the dominant source of the spin-orbit interaction.

Because silicon is characterized by weak spin-orbit interaction, it has not been considered as a candidate for the SpinFET channel material. Recently, however, it was shown (8) that thin silicon films in SiGe/Si/SiGe heterostructures can have large values of spin-orbit interaction. Interestingly, the Rashba spin-orbit interaction is relatively weak; its strength is approximately ten times smaller than the value of the dominant contribution which is of the Dresselhaus type with the corresponding effective Hamiltonian in the form

$$H_R = \frac{\beta}{\hbar}(p_x\sigma_x - p_y\sigma_y), \qquad [3]$$

This major contribution to the spin-orbit interaction is due to interfacial-induced disorder which breaks the inversion symmetry. It depends almost linearly on the effective electric field (9). For a built-in field of 50kV/cm, the strength of the Dresselhaus spin-orbit interaction is found to be $\beta \approx 2\mu eVnm$, which is in agreement with the value reported experimentally (10), while $\alpha_R \approx 0.1\mu eVnm$. The value of the Dresselhaus spin-orbit interaction in confined silicon systems is sufficient to consider them for applications in SpinFET channels.

The stronger spin-orbit interaction leads to an increased spin relaxation. The D'yakonov-Perel' mechanism is the main spin relaxation mechanism in the systems with the effective spin-orbit interaction [2,3]. In quasi-one-dimensional electron structures, however, a suppression of the spin relaxation mechanism is expected (11). Indeed, in case of elastic scattering only back-scattering is allowed. Reversal of the electron momentum results in the inversion of the effective magnetic field direction. Therefore, the precession angle does not depend on the number of scattering events along the carrier trajectory in the channel, but is a function of the channel length only. Thus, the spin-independent elastic scattering does not result in additional spin decoherence. In the presence of an external magnetic field, however, spin-flip processes become possible, and the Elliott-Yafet spin relaxation mechanism must also be considered (12).

Model

To calculate the transport properties of the ballistic spin field-effect transistor we consider a model similar to (12) and (13). The Hamiltonian in the ferromagnetic regions has the following form in the one-band effective mass approximation:

$$H = \frac{p_x^2}{2m_f^*} + h_0\sigma_z, \quad x < 0, \qquad [4]$$

$$H = \frac{p_x^2}{2m_f^*} \pm h_0\sigma_z, \quad x > L, \qquad [5]$$

where m^*_f is the effective mass in the contacts, $h_0=2PE_F/(P^2+1)$ is the exchange splitting energy with P defined as the spin polarization in the ferromagnetic regions, E_F is the Fermi energy, and σ_z is the Pauli matrix; ± in [5] stands for the parallel and anti-parallel configuration of the contact magnetization. For the semiconductor region the Hamiltonian reads (12), (13)

$$H = \frac{p_x^2}{2m_s^*} + \delta E_c - \frac{\alpha_R}{\hbar}\sigma_y p_x + \frac{1}{2}g\mu_B B\sigma^*, \qquad [6]$$

where m^*_s is the subband effective mass, δE is the band mismatch between the ferromagnetic and the semiconductor region, g is the Landé factor, μ_B is the Bohr

magneton, B is the magnetic field, and $\sigma^* \equiv \sigma_x\cos\gamma + \sigma_y\sin\gamma$ with γ defined as the angle between the magnetic field and the transport direction.

To calculate the dependence of the transport properties on the spin-orbit interaction we need the electron eigenfunctions. For the ferromagnetic regions the spin-up and spin-down eigenstates have the form $(1, 0)^\dagger$ and $(0, 1)^\dagger$, respectively. The wave function in the left contact has the following form:

$$\Psi_L(x) = (e^{ik_\uparrow x} + R_\uparrow e^{-ik_\uparrow x})\begin{pmatrix}1\\0\end{pmatrix} + R_\downarrow e^{-ik_\downarrow x}\begin{pmatrix}0\\1\end{pmatrix}, \quad [7]$$

$$\Psi_L(x) = R_\uparrow e^{-ik_\uparrow x}\begin{pmatrix}1\\0\end{pmatrix} + (e^{ik_\downarrow x} + R_\downarrow e^{-ik_\downarrow x})\begin{pmatrix}0\\1\end{pmatrix}, \quad [8]$$

where [7] represents the incoming spin-up electrons and [8] the incoming spin-down electrons, correspondingly, $k_{\uparrow(\downarrow)} = \sqrt{2m_f^*(E \mp h_0)/\hbar^2}$ is the wave vector of the spin-up (spin-down) electron and $R_{\uparrow(\downarrow)}$ is the amplitude of the reflected wave. For the right contact the wave function is given by

$$\Psi_R(x) = C_\uparrow e^{ik_\uparrow x}\begin{pmatrix}1\\0\end{pmatrix} + C_\downarrow e^{ik_\downarrow x}\begin{pmatrix}0\\1\end{pmatrix}. \quad [9]$$

For the semiconductor region the wave function can be written as

$$\Psi_S(x) = A_+ e^{ik_{x1}^{(+)}x}\begin{pmatrix}k_1\\1\end{pmatrix} + B_+ e^{ik_{x2}^{(+)}x}\begin{pmatrix}k_2\\1\end{pmatrix} + A_ e^{ik_{x1}^{(-)}x}\begin{pmatrix}k_3\\-1\end{pmatrix} + B_ e^{ik_{x2}^{(-)}x}\begin{pmatrix}k_4\\-1\end{pmatrix}, \quad [10]$$

where $k_{x1(x2)}^{(+)}$ and $k_{x1(x2)}^{(-)}$ are the wave vectors obtained by solving the equations $\frac{\hbar^2 k^2}{2m_s^*} + \delta E_c \pm \sqrt{\left(\frac{Bg\mu_B\cos(\gamma)}{2}\right)^2 + \left(\frac{Bg\mu_B\sin(\gamma)}{2} - \alpha_R k\right)^2} = E,$ respectively.

The constants k_1, k_2, k_3, and k_4 are calculated as

$$k_1 = -\frac{i\left(Bg\mu_B\sin(\gamma) - 2\alpha_R k_{x1}^{(+)}\right) - Bg\mu_B\cos(\gamma)}{2\sqrt{\left(\frac{Bg\mu_B\cos(\gamma)}{2}\right)^2 + \left(\frac{Bg\mu_B\sin(\gamma)}{2} - \alpha_R k_{x1}^{(+)}\right)^2}}, \quad [11]$$

$$k_2 = -\frac{i\left(Bg\mu_B\sin(\gamma) - 2\alpha_R k_{x2}^{(+)}\right) - Bg\mu_B\cos(\gamma)}{2\sqrt{\left(\frac{Bg\mu_B\cos(\gamma)}{2}\right)^2 + \left(\frac{Bg\mu_B\sin(\gamma)}{2} - \alpha_R k_{x2}^{(+)}\right)^2}}, \quad [12]$$

$$k_3 = \frac{i\left(Bg\mu_B \sin(\gamma) - 2\alpha_R k_{x1}^{(-)}\right) - Bg\mu_B \cos(\gamma)}{2\sqrt{\left(\frac{Bg\mu_B \cos(\gamma)}{2}\right)^2 + \left(\frac{Bg\mu_B \sin(\gamma)}{2} - \alpha_R k_{x1}^{(-)}\right)^2}}, \quad [13]$$

$$k_4 = \frac{i\left(Bg\mu_B \sin(\gamma) - 2\alpha_R k_{x2}^{(-)}\right) - Bg\mu_B \cos(\gamma)}{2\sqrt{\left(\frac{Bg\mu_B \cos(\gamma)}{2}\right)^2 + \left(\frac{Bg\mu_B \sin(\gamma)}{2} - \alpha_R k_{x2}^{(-)}\right)^2}}. \quad [14]$$

The reflection and transmission coefficients are determined by applying the boundary conditions at the ferromagnet/semiconductor interfaces.

We compute the current through the device as

$$I^{P(AP)}(V) = \frac{e}{h}\int_{\delta E_c}^{\infty}\left[T_\uparrow^{P(AP)}(E) + T_\downarrow^{P(AP)}(E)\right]\left\{\frac{1}{1+e^{\frac{E-E_F}{k_B T}}} - \frac{1}{1+e^{\frac{E-E_F+eV}{k_B T}}}\right\}dE, \quad [15]$$

where k_B is the Boltzmann constant, T is the temperature, and V is the voltage. The spin-up ($T^P{}_\uparrow$) and spin-down ($\mathrm{T}^{\mathrm{P}}{}_\downarrow$) transmission probability for the parallel configuration of the contact magnetization is defined as

$$T_\uparrow^P = \left|C_\uparrow\right|^2 + \frac{k_\downarrow}{k_\uparrow}\left|C_\downarrow\right|^2, \quad [16]$$

$$T_\downarrow^P = \frac{k_\uparrow}{k_\downarrow}\left|C_\uparrow\right|^2 + \left|C_\downarrow\right|^2. \quad [17]$$

For the anti-parallel configuration of contact magnetization the transmission probability is obtained in the same way.

The conductance is defined as

$$G^{P(AP)} = \lim_{V\to 0}\frac{I^{P(AP)}}{V}. \quad [18]$$

In the limit of low temperature the conductance must coincide with the one obtained from the Laudauer-Büttiker formula

$$G^{P(AP)} = \frac{e^2}{h}\left(T_\uparrow^{P(AP)}(E_F) + T_\downarrow^{P(AP)}(E_F)\right). \quad [19]$$

Finally, the magnetoresistance (TMR) is defined as

$$TMR \equiv \frac{G_P - G_{AP}}{G_{AP}}. \qquad [20]$$

Results and Discussion

In our calculations we use two types of materials for the semiconductor region: InAs, which is characterized by a strong value of the spin-orbit interaction, and silicon, which is characterized by a moderate value of the spin-orbit interaction.

InAs Calculations

For all the calculations for the InAs semiconductor channel we assume the effective mass for the ferromagnetic region $m_f^* = m_0$ and for the semiconductor region $m_s^* = 0.036m_0$, where m_0 is the electron rest mass. Figure 1 shows the dependence of the TMR on the value of the band mismatch δE_c between the ferromagnetic source contact and the semiconductor channel. The TMR oscillates between positive and negative values. As the length of the semiconductor channel decreases, the period of the oscillations increases roughly proportionally to the inverse length of the semiconductor channel.

Temperature exerts a significant influence on the device characteristics as shown in Figure 2. For a channel length $L = 0.05$µm the oscillatory amplitude of the TMR decreases for $T = 25$K and completely vanishes for $T = 150$K. The reason for the oscillatory behavior to disappear at $T = 150$K is a relatively short period of the conductance oscillations (and correspondingly TMR oscillation shown in Figure 1) with respect to δE_c. Thus one can expect that for the shorter channel the oscillatory amplitude could be sufficient to modulate the current in the SpinFET at elevated temperatures.

The current dependence on the value of the drain-source voltage is shown in Figure 3. A clear S-like shape of the curves is observed at $T = 10$K. This is a manifestation of the conductance oscillations as a function of δE, which have a large amplitude due to the presence of the delta-function barriers at the interfaces between the contact and the channel ($z = 3$). A large amplitude of the conductance oscillations guarantees the different slopes of the IV curves corresponding to different δE_c. Although the S-like non-linearity is not well pronounced at elevated temperatures, the difference in the slopes at small voltages is not completely washed out, even at room temperature.

Si Calculations

We consider square silicon fins of [100] and [110] orientations, with (001) horizontal faces. The spin-orbit interaction is taken in the Dresselhaus form [3]. The dependence of the TMR on the spin-orbit interaction is shown in Figure 4. The wave vector $k_D = m_S\beta/\hbar^2$ determines the dependence of the TMR on the value of the strength of the Dresselhaus spin-orbit interaction β. Fins with [100] orientation posses a larger subband effective mass (14) compared to [110] oriented fins. Therefore, a smaller variation of β is required in [100] oriented fins to achieve the same variation of k_D and thus the same variation of TMR.

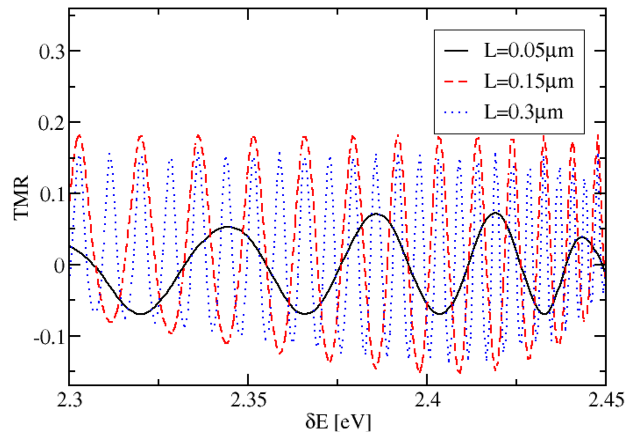

Figure 1. TMR dependence on the value of δE for α_R = 42.3meVnm, E_F = 2.47eV, P = 0.4, B = 0T, z = 0.

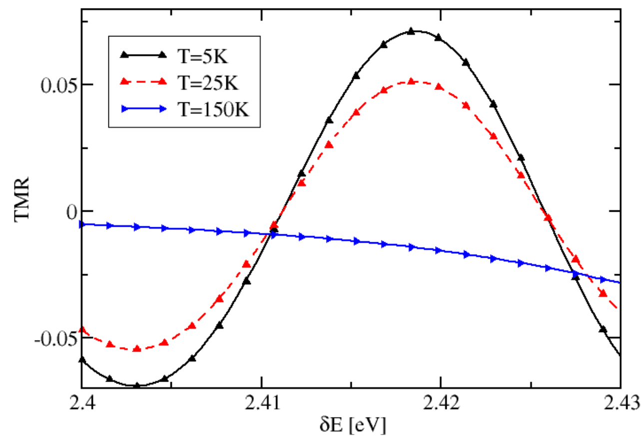

Figure 2. TMR dependence on the value of δE for α_R = 42.3meVnm, E_F = 2.47eV, P = 0.4, B = 0T, z = 0, L = 0.05µm.

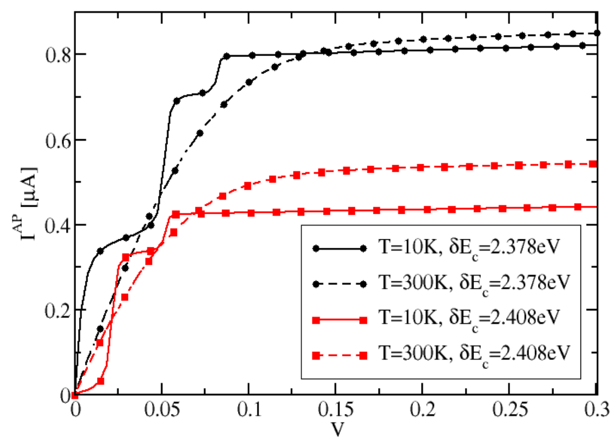

Figure 3. Current dependence on the value of the drain-source voltage for B = 0T, z = 3, L = 0.03µm, P = 0.4.

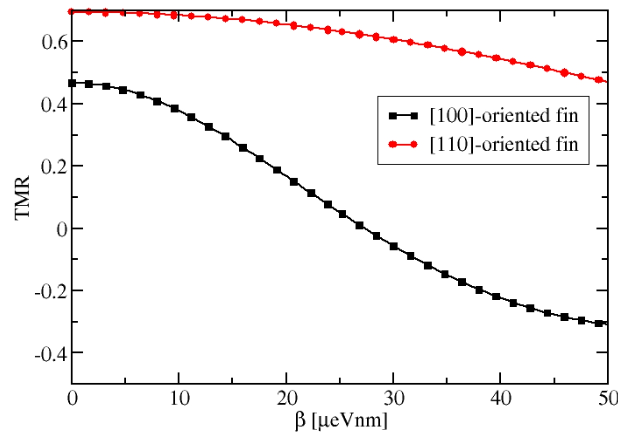

Figure 4. TMR dependence in a silicon SpinFET on the value of the Dresselhaus spin-orbit interaction for $P = 0.6$, $z = 2$, $L = 5\mu m$.

Summary and Conclusion

A small semiconductor channel length provides a possibility to create a SpinFET which will operate at room temperature. Silicon fins with [100] orientation are best suitable for practical realization of silicon-based SpinFETs.

Acknowledgments

This work is supported by the European Research Council through the grant #247056 MOSILSPIN.

References

1. S. Datta and B. Das, *Appl. Phys. Lett.*, **56**, 665 (1990).
2. S. Sugahara and J. Nitta, *Proceedings of the IEEE*, **98**, No.12, (2010).
3. J. Cheng *et al., Phys. Rev. Lett.* **104**, 016601 (2010).
4. S. Dash *et al.,* arXiv:1101.1691 (2011).
5. B. Huang *et al., Phys. Rev. Lett.* **99**, 177209 (2007).
6. E. I. Rashba, *Fiz.Tver. Tela (Solid State Physics USSR), vol. 2.*, p.1109, (1960).
7. G. Dresselhaus, *Phys. Rev.* **100**, pp.580-586 (1955).
8. M. Nestoklon *et al., Phys. Rev.*, B **77**, 155328 (2008).
9. M. Prada *et al., New J.Phys.*, **13**, 013009 (2011).
10. Z. Wilamowski and W. Jantsch, *Phys. Rev. B*, **69**, 035328 (2004).
11. A. Bournel *et al.*, *European Phys. J. Appl. Phys.*, **4**, 1 (1998).
12. M. Cahay and S. Bandyopadhyay, *Phys. Rev. B*, **69**, 045303 (2004).
13. K. Jiang *et al.*, *IEEE Transactions on Electron Devices,* **57**, 2005 (2010).
14. H. Tsuchiya *et al.*, *IEEE Transactions on Electron Devices,* **57**, 406 (2010).